JOURNAL OF MATERIALS SCIENCE **35** (2000) 889–894

Effects of shear rate and particle concentration on rheological properties of magnetic particle suspensions

H. J. CHOI*
Department of Polymer Science and Engineering, Inha University, Inchon, 402-751, Korea
E-mail: hjchoi@inha.ac.kr

T. M. KWON, M. S. JHON
Department of Chemical Engineering, Carnegie Mellon University, Pittsburgh, PA 15213, USA

Rheological characterizations were made for various types of magnetic particles (rod-like γ-Fe_2O_3, CrO_2, and plate-like Ba-ferrite) and nonmagnetic (rod-like α-Fe_2O_3) suspensions, in terms of particle concentration and shear rate. Shear rate dependence on viscosity was accurately described by the Casson equation. The highest yield stress for Ba-ferrite among the four types of particles represents the sensitive flocculation characteristics of Ba-ferrite with respect to concentration. The effect of non-magnetic α-Fe_2O_3 and magnetic γ-Fe_2O_3 particle mixtures on suspension viscosity was also examined, and a negative deviation from the tie line of individual particle viscosities was observed.

1. Introduction

Magnetic recording media, such as magnetic tapes and floppy disks, consist of a coating of fine magnetic particles on a non-magnetic plastic substrate. The final product is greatly affected by the dispersion quality of the magnetic particle suspensions [1]. Although the particulate media industries are mature, an unsolved problem of dispersion quality, which plagues coating processes involving unstable particle suspensions, still remain.

It is well known that, when magnetic particles are immersed in a fluid, there is a dynamic coupling between the fluid and the particles [2]. Suspended particles perturb the fluid media, while from Newton's third law, the fluid also changes the particle dynamics. This dynamic coupling is experimentally observable, either by studying the overall suspension behavior or by examining the dynamics of the particle orientations. The overall suspension properties exhibit non-Newtonian behavior [3], and this effect can be measured by standard rheological devices.

However, despite numerous studies on the physicochemical aspects of particle suspensions [4–7], not many studies address the rheological characterization of single-domain magnetic particle suspensions. By measuring the thixotropic behavior of Fe_3O_4 particles in a dioctyl adipate solvent, Mehta *et al.* [8] observed shear stress hysteresis. They also presented a certain decay of shear stress with imposition time of shear. For γ-Fe_2O_3 particles in silicone oil, Yang *et al.* [9] observed flow instabilities occurring over a shear rate range of $\dot{\gamma} = 0.1$–$1.0\ \text{sec}^{-1}$ from shear stress-shear rate behavior and also found an agreement between the experimentally-observed yield stress values and those obtained by fitting stress-shear rate data with the Casson equation. Kuin [10] measured rheological properties of CrO_2 and γ-Fe_2O_3 particle suspensions and also developed a theory for the viscoelastic deformation of magnetic particle suspensions. By fitting shear stress versus shear rate data to his theory, Kuin obtained rheological properties such as yield stress, shear viscosity, and relaxation time for elastic deformation. He also demonstrated that these parameters are useful measures of the flocculation state of a suspension by revealing the dependence of these parameters on milling time. From his results, viscosity decreased with milling time, while the other three parameters had a minimum value for a certain milling time.

Dasgupta [11, 12] further performed rheological measurements and, in parallel, examined the sedimentation and magnetic recording performance of the magnetic particle suspensions in terms of surfactant level, concentration, and milling time. He inferred that the addition of surfactants resulted in better dispersion quality and stability such as a decrease in suspension viscosity, an increase in sedimentation time, squareness and orientation ratio, and a narrowing switching field distribution.

Jhon *et al.* [13] studied the microstructural state of magnetic particle suspensions by adopting two different microrheological characterization techniques with

* Author to whom all correspondence should be addressed.

rheomagnetic and rheooptic measurements. They found that the techniques complement one another by measuring the order parameter for the magnetic particles in suspension over different concentration ranges. That is, the rheomagnetic measurement [14–16] is effective for on-line characterization of microrheological properties of concentrated magnetic particle suspensions, and the rheooptical measurement [17, 18] is useful for off-line dispersion microstates and rheological properties of the dilute suspensions.

As a continuation of our previous study [19, 20], we study the effects of microstructure on the measured viscosity of suspensions of rod-like magnetic γ-Fe_2O_3 and CrO_2, rod-like nonmagnetic α-Fe_2O_3, and plate-like Ba-ferrite particles. When flocs in suspension undergo shearing motion, loose floc structures will deform and progressively break up into smaller flocs, releasing the immobilized fluid. As a consequence, both the hydrodynamic volume of the dispersed phase and viscosity are reduced. Further increase in shear rate will ultimately lead to breaking up of all the flocs into primary particles. If the imposed shear is removed, the particles will reflocculate. The breakdown and reflocculation of flocs is considered a reversible process. Hence, at a certain shear rate, there is an equilibrium or steady-state distribution of microstructures in suspension where the steady-state viscosity can be obtained. The steady-state viscosity is shear-rate dependent due to the equilibrium dependence on shear rate. For a suddenly-imposed shear, a finite time is required to establish a steady-state. Therefore, the viscosity of the flocculated suspension is normally dependent upon both time and shear rate.

2. Experimental

The magnetic particles used in this study were the single-domain particles described in our previous paper [19]. Both rod-like magnetic γ-Fe_2O_3 particles and non-magnetic α-Fe_2O_3 particles were obtained from Magnox Co. Because the α-Fe_2O_3 were thermally treated to simply manufacture the γ-Fe_2O_3 particles, the size and shape of these two types of particles were nearly the same. Rod-like CrO_2 particles and plate-like Ba-ferrite particles were obtained from Dupont Co. and Toda Co. (Japan), respectively. Note that, in contrast to rod-like particles, the direction of spontaneous magnetization of plate-like Ba-ferrite is normal to the face of the platelets.

The size and shape of the particles were characterized using a transmission electron microscope. The magnetic properties of particles for randomly-oriented dry powders were measured by a vibrating sample magnetometer. The particle density was calculated using the volume increase when a known mass of particles was immersed into a fluid. The physical properties of the magnetic particles are listed in Table I.

The sample preparation method and the rheological measurement were the same as previously described [19]. A 150 ml master solution of each magnetic suspension having an approximate volume fraction of 0.05 was prepared by mixing the particle powder with ethylene glycol and then passing the suspension twice through a mini-Eiger motor mill at a speed of 1000 rpm

TABLE I Physical properties of the magnetic particles

Property	Rod-like			Plate-like
	γ-Fe_2O_3	α-Fe_2O_3	CrO_2	Barium-ferrite
M_s (emu g^{-1})	71.8	—	81.49	34.97
H_c (Oe)	321	—	585	635
Density ρ_p (g cm^{-3})	4.7	4.7	4.8	5.2
Particle size[a] (μm)	$L = 0.5$	$L = 0.5$	$L = 0.46$	$a = 0.13$
Aspect ratio $= L/a$	7.0	7.0	13	0.1
Curie temp. T_c (°C)	590	—	115–126	320

According to the vendor's note, the α-Fe_2O_3 particles were thermally treated to manufacture γ-Fe_2O_3 particles, and therefore, the size and shape of these two types of particles were identical.
[a] L, length of the particle; a, diameter of the particle.

[16]. More dilute samples were prepared by subsequent dilution of the concentrated master suspension.

For viscosity measurements, the Wells-Brookfield LVT-D cone and plate viscometer with the C-42 cone type was used. The plate served as a sample cup with a built-in circulation channel and ports for a recirculant from a constant temperature bath. This specific cone and plate combination is designed to incorporate approximately 1 ml of sample. The viscometer has a torque meter which can be driven at eight discrete rotational speeds ranging from 0.3 to 60 rpm with a corresponding shear rate range of 1.15 to 230 sec^{-1}. To maintain a constant temperature during the measurement, the jacket ports in the sample cup were connected to a recirculating loop of a constant temperature bath. All measurements were performed at 25°C. For automatic data acquisition, the signal output receptacle of the viscometer and the thermocouples were multiplexed to a voltmeter, which is interfaced to an IBM personal computer via a GPIB bus.

Preceding each test, approximately 1 ml of suspension sample was introduced into the sample cup using a precision pipette. Great care was taken to maintain a consistency in sampling, because fluctuation in the sampling is a critical factor to reproducibility of the measurement. After setting the viscometer, the test suspension is sheared for 3 minutes at a maximum test shear rate of 115 sec^{-1} (30 rpm) to obtain a homogeneous dispersion, after which the suspension was stabilized for 2 minutes. After stabilization, the suspension was sheared at the highest test shear rate for 2 minutes, and then 20 measurements were performed in 5-second-intervals. A steady-state viscosity was obtained by averaging the measured values.

3. Results and discussion

From the rheological measurements for various types of magnetic particle suspensions, preliminary insight into the rheological characterization of the magnetic particle suspensions from fitting experimental observations with theory was obtained. Furthermore, the effects of particle concentration, shear rate, and particle mixture on measured viscosity were investigated.

A typical rheological characteristic of particle suspensions containing flocs is shear thinning [6]. When an external shear stress is imposed, some loose flocs

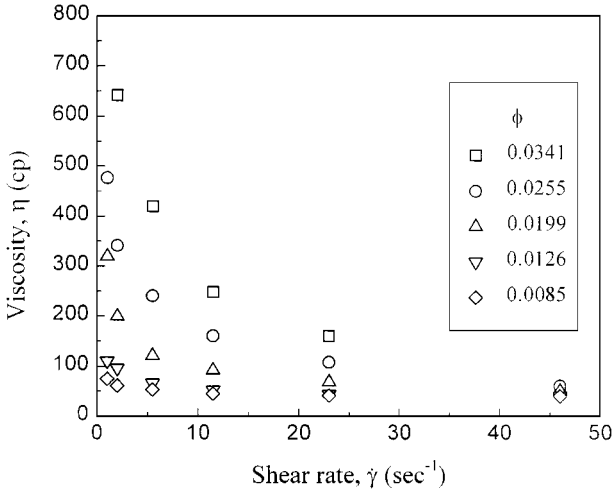

Figure 1 Viscosity as function of shear rate for CrO_2 particle suspensions of various particle concentrations.

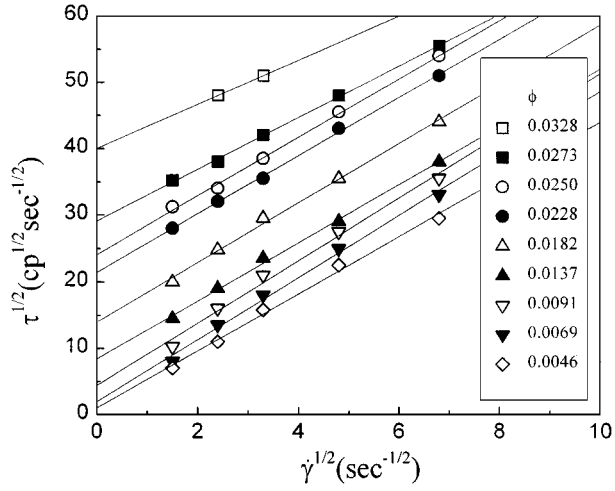

Figure 2 $\tau^{1/2}$ versus $\dot{\gamma}^{1/2}$ plot for γ-Fe_2O_3 particle suspensions.

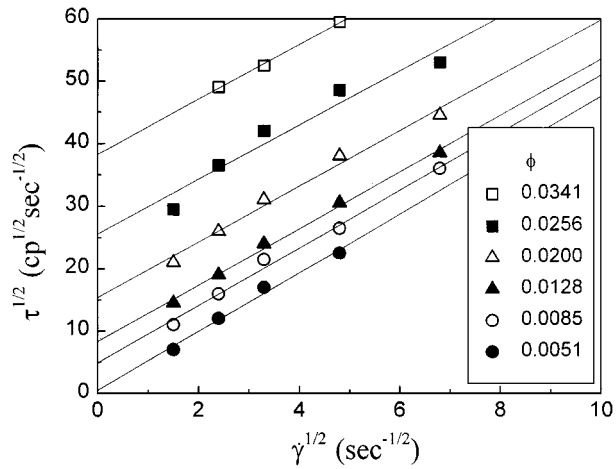

Figure 3 $\tau^{1/2}$ versus $\dot{\gamma}^{1/2}$ plot for CrO_2 particle suspensions.

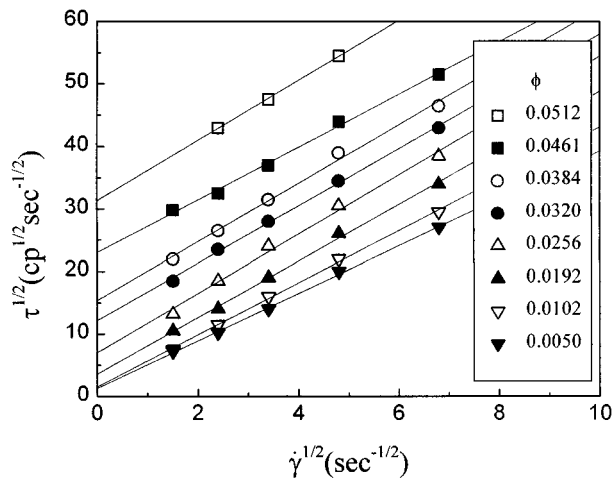

Figure 4 $\tau^{1/2}$ versus $\dot{\gamma}^{1/2}$ plot Ba-ferrite particle suspensions.

deform to structures, which require less viscous dissipation. At a higher shear stress, the flocs break into smaller or primary structures, consequently releasing a certain amount of the immobilized liquid. This effect results in a decrease in suspension viscosity with shear rate. For non-spherical particle suspensions, however, the situation is more complicated. Hydrodynamic theory predicts that the viscosity of non-spherical particle suspensions is higher than that of spherical particle suspensions, and therefore breakdown of spherical flocs into non-spherical particles by shear leads to increased suspension viscosity. Hence, the two effects are competing with each other [19]. As illustrated in Fig. 1, magnetic particle suspensions typically showed the shear-thinning behavior, implying that the former effect is dominant.

In describing the time independent viscosity, the most widely used empirical model was developed by Casson [21]. He considered that rigid primary particles flocculate into rod-like structures and developed an expression for the tension in rods under flow. The rods break when the tension exceeds a critical value. With increasing shear rate, the length of the rods will progressively be reduced until the rods are completely broken down into primary particles at very high shear rates. On the basis of this reasoning, the relationship between the shear stress (τ) and shear rate ($\dot{\gamma}$) becomes:

$$\tau^{1/2} = \tau_0^{1/2} + \eta_\infty^{1/2}\dot{\gamma}^{1/2}. \qquad (1)$$

here, τ_0 is the yield stress and η_∞ is the suspension viscosity at infinite shear rate. Equation 1 is known as Casson's equation, used for the shear rate dependence of the suspension viscosity, and it will be used to analyze the our data.

In order to investigate the shear rate dependence on viscosity, we fitted the measured viscosity to the Casson equation given by Equation 1. Typical results are presented in Figs 2–5 for γ-Fe_2O_3, CrO_2, Ba-ferrite and α-Fe_2O_3 particle suspensions, respectively. For all four types of particle suspensions, Equation 1 agreed well with the measured viscosity. The curves clearly indicate that a finite yield stress value exists for the magnetic particle suspensions, and as the particle concentration decreases, the intercept related to yield stress approaches zero, i.e., the Newtonian fluid limit. In addition, the slope of the curve is related to the viscosity at infinite shear rate. The existence of an apparent yield stress is not surprising; previous investigators [3, 9] have reported similar observations, and this phenomenon is mainly attributed to interparticle forces. Figs 2–5 also illustrate that highly dilute particle

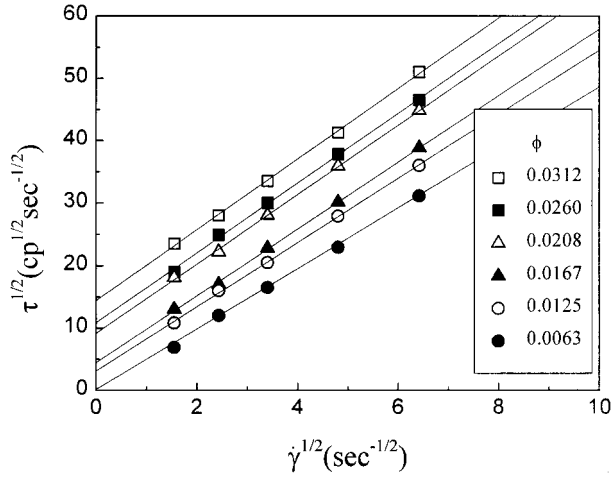

Figure 5 $\tau^{1/2}$ versus $\dot{\gamma}^{1/2}$ plot for α-Fe_2O_3 particle suspensions.

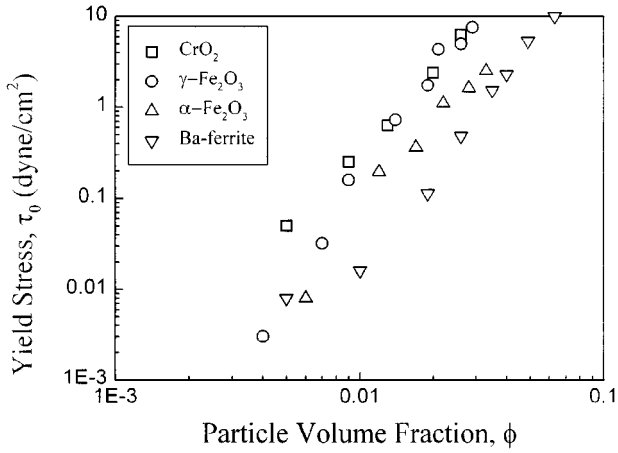

Figure 6 Yield stress τ_0 dependence on particle volume fraction ϕ for various magnetic and non-magnetic particles.

suspensions ($\phi < 0.01$) still exhibit the existence of small, but finite, yield stresses. This implies that the particles in suspension still exist as flocs in the dilution regime, which is consistent with the observation made by Bottoni *et al.* [22] using an optical microscope. From Figs 2–5, we calculated η_∞ (slope) and τ_0 (intercept).

Fig. 6 shows the τ_0 dependence on particle volume concentration (ϕ) for various types of particles. For all particle suspensions, the yield stress increased with particle concentration. This phenomenon is evident since, as particle concentration increases, the distance between particles is reduced and interparticle interactions increase, which can lead to formation of more interlinked structures. The absolute magnitudes of the yield stress values are shown to be the largest for CrO_2 and γ-Fe_2O_3 particles and smallest for Ba-ferrite. The smaller magnitude of the yield stress for nonmagnetic α-Fe_2O_3 relative to that of magnetic γ-Fe_2O_3 indicates that the magnetic interaction is significant and is consistent with the observation made by Smith and Bruce [3]. For all particle suspensions, in a concentration range of $0.01 < \phi < 0.05$, the dependence of the yield stress on particle volume concentration is almost linear on a log-log plot, as shown in Fig. 6. This implies that the yield stress dependence on particle concentration becomes:

$$\tau_0 \propto \phi^b, \tag{2}$$

where the exponent b is a measure of the incremental increase in interparticle interactions and flocculation with concentration. The linearity of the yield stress versus particle concentration curve (log-log plot) implies that particle flocculation occurs in a consistent manner in this concentration range. In the sufficiently dilute concentration regime, however, the yield stress deviates from the linearity due to changes in the flocculation behavior. In Fig. 6, however, the flocculation behavior in the dilute concentration region ($\phi < 0.01$) can not be clearly seen due to precision limitations of our viscometer. Values of the exponent b for various types of particles in the concentration range $0.01 < \phi < 0.05$ were obtained: 1.77 for γ-Fe_2O_3, 1.59 for α-Fe_2O_3, 1.64 for CrO_2, and 1.96 for Ba-ferrite particles. The largest value for Ba-ferrite among the four different types of particles implies that interparticle interactions and flocculation of the Ba-ferrite particles increase most dramatically as the distance between particles becomes smaller. The smallest magnitude for nonmagnetic α-Fe_2O_3 seems to suggest the formation of relatively loose structures compared to similarly-shaped magnetic particles.

From the slope of the Casson equation fit illustrated in Figs 2–5, we also obtained the intrinsic viscosity at infinite shear rate $[\eta]_\infty$ for various particle concentrations, and the results are presented in Fig. 7. For all types of particle suspensions, $[\eta]_\infty$ ranged from 3 to 80 and showed a decreasing trend with particle concentration. One may expect the intrinsic viscosity at infinite shear rate to increase with particle concentration. This apparent conflict can be attributed to an error related to the sensitivity of the curve fitting, which is similar to what we encountered in determining ϕ_∞ from Mooney's equation (given in Equation 3).

In Mooney's development, the relative viscosity of a suspension $\eta(\phi)$ is expressed by $\eta(\phi)/\eta(\phi = 0) = H(\phi)$ with $H = \exp[2.5\phi/(1 - K\phi)]$ as a solution for spherical particle suspensions, where K is the "crowding factor". A straightforward extension of his expression for a spheres yields an expression for non-spherical particles:

$$\ln\left(\frac{\eta(\phi)}{\eta(\phi = 0)}\right) = \frac{[\eta]\phi}{1 - \phi/\phi_\infty}. \tag{3}$$

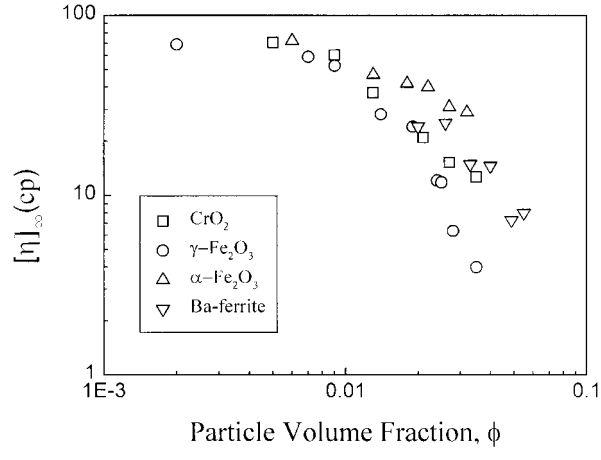

Figure 7 Dependence of the intrinsic viscosity at infinite shear rate $[\eta]_\infty$ on volume fraction ϕ for various magnetic and non-magnetic particles.

In order to obtain information on the state of the suspension over a given concentration range, the measured viscosity is fitted with predictions incorporating concentration effects. Two parameters, $[\eta]$ and ϕ_∞, are determined from fitting the experimental data with theory. With the Mooney equation given by Equation 3, the curve fitting parameters, $[\eta]$ and ϕ_∞, are determined from the intercept, $-[\eta]^{-1}\,\phi_\infty^{-1}$, and the slope $[\eta]^{-1}$ on the $1/\ln[\eta(\phi)/\eta(\phi=0)]$ versus ϕ^{-1} curve. In Figs 2–5, there is a very small difference of $O\,(10^{-1})$ between the slopes of different concentrations, and precise determination of this small difference is very difficult with limited data. However, small errors in determining the slope yields a fatal error in $[\eta]_\infty$, since $[\eta]_\infty$ is obtained after being divided by ϕ (typically $\phi \ll 1$).

Yang *et al*. [9] observed that the intrinsic viscosity fluctuates around $[\eta]_\infty = 12$–13 for $\phi = 0.024$–0.087 and increases to $[\eta]_\infty = 23$ for $\phi = 0.129$ for γ-Fe_2O_3 particle suspensions using a precision rheometer. Thus, it seems difficult to accurately determine $[\eta]_\infty$ from the Casson equation fit in the practical concentration range of $0.01 < \phi < 0.1$. This is more apparent from the results obtained by Smith and Bruce [3], where $[\eta]_\infty$ was shown to increase with concentration when the data were fitted to a Mooney-type equation, but the opposite trend occurred in the fit with the Casson equation. This opposite intrinsic viscosity trend occurs since the point of emphasis is different between the Mooney type and the Casson equations; the Mooney equation is more concerned with viscous effects, while the Casson equation is more elaborate with the elastic properties (yield stress) of the suspensions. Some approaches attempted to combine these two effects [23]. However, this procedure seems to eventually result in the incorporation of extra fitting parameters into the theory. Therefore, the intrinsic viscosity values determined by the Casson equation fit seem to have little practical or reliable importance.

Following Smith and Bruce [3], $[\eta]_\infty$ can be obtained as an asymptotic value of the intercept in the $[\eta]$ versus $\dot\gamma^{-1/2}$ curve at infinite shear rate. The values of $[\eta]$ obtained by fitting Mooney's equation are plotted in Fig. 8. Due to limited data, it is difficult to accurately define this asymptotic behavior. However, a linear dependence of the intrinsic viscosity on $\dot\gamma^{-1/2}$ can be observed in the region of $\dot\gamma^{-1/2} < 0.2$–$0.3\ \mathrm{sec}^{1/2}$. A rough evaluation of the intercept gave values of $[\eta]_\infty = 26$ for CrO_2 and γ-Fe_2O_3, $[\eta]_\infty = 22$ for α-Fe_2O_3, and $[\eta]_\infty = 12$ for Ba-ferrite. Compared to the hydrodynamic theory predictions shown in Fig. 7 of Kwon *et al*. [19], these values are unrealistically high, partially due to high intrinsic viscosity values estimated from the equation fitting and an extrapolation of data obtained in an apparently low shear rate region. However, the obtained values of $[\eta]_\infty$ seem to reflect characteristics of the different types of particles; since the particles in suspension would exist as primary particles at infinite shear rate, whereas the largest value of $[\eta]_\infty$ for both CrO_2 and γ-Fe_2O_3 is characteristic of rod-like magnetic particles, the slightly lower value of α-Fe_2O_3 corresponds to rod-like but non-magnetic properties, and the smallest value for Ba-ferrite is due to its plate-like shape.

We also performed the rheological measurements for mixtures [16] of nonmagnetic α-Fe_2O_3 and magnetic γ-Fe_2O_3 particle suspensions. The measured viscosity dependence of γ-Fe_2O_3 suspensions on various levels of α-Fe_2O_3 is presented in Fig. 9 for total particle volume fraction $\phi_t = 0.025$ and in Fig. 10 for $\phi_t = 0.020$.

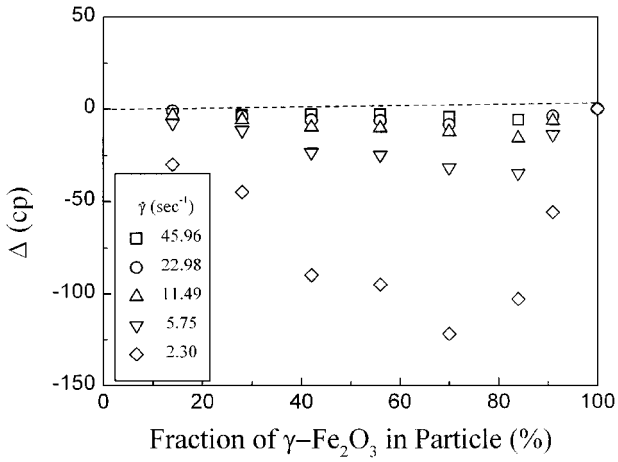

Figure 9 Deviation of viscosity for mixture suspensions of nonmagnetic α-Fe_2O_3 and magnetic γ-Fe_2O_3 at total concentration $\phi_t = 0.025$.

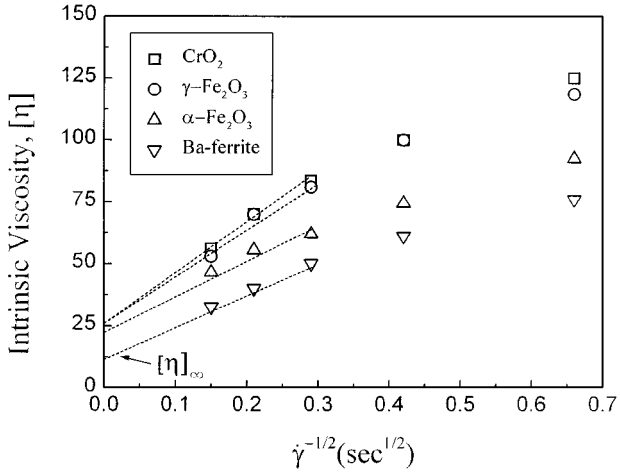

Figure 8 Intrinsic viscosity $[\eta]$ versus $\dot\gamma^{-1/2}$ for various magnetic and non-magnetic particles by fitting Mooney's equation.

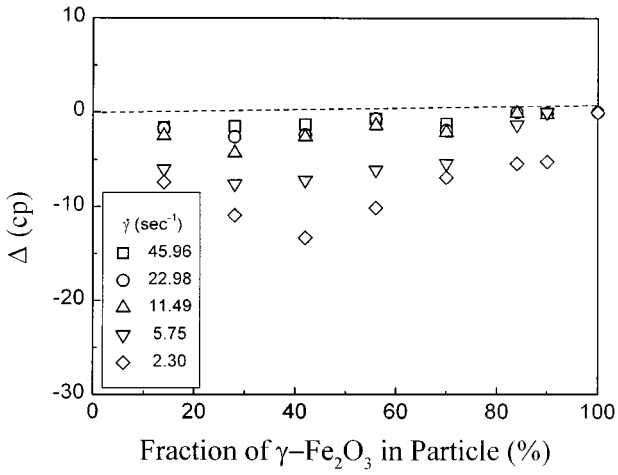

Figure 10 Deviation of viscosity for mixture suspensions of nonmagnetic α-Fe_2O_3 and magnetic γ-Fe_2O_3 at total concentration $\phi_t = 0.020$.

Here, deviation from the tie line of individual particle viscosities, Δ, is defined as $\Delta = \eta_{\text{mix}} - (\eta_1\phi_1/\phi_t + \eta_2\phi_2/\phi_t)$, where η_{mix} and η_i $(i = 1, 2)$ are the viscosities of the particle mixture and pure i-particle suspensions, and $\phi_t = \phi_1 + \phi_2$ is the total particle volume concentration in the mixture suspension. The mixture suspensions showed $\Delta < 0$ from the tie line of the individual particle viscosities. The absolute magnitude of Δ was largest at the lowest shear rate and gradually flattened out as the shear rate increased. This flattening is due to shear thinning of the suspension. The negative value of Δ for the mixture can be ascribed to two effects in terms of suspension state: one is that both the decreased interparticle interaction of magnetic γ-Fe_2O_3, due to nonmagnetic α-Fe_2O_3 and the increased orientability of α-Fe_2O_3 due to magnetic γ-Fe_2O_3 led to reduction in viscosity. The other explanation arose from observations by Chong *et al*. [24] and Farris [25]. They demonstrated that the overall viscosity of polydisperse particle suspensions exhibits $\Delta < 0$ and that the magnitude of Δ also increases as the polydispersity index increases. Thus, the polydispersity effect is responsible for the observation of $\Delta < 0$ in Figs 9 and 10. As shear rate increases, the large loose flocs deform and break up to form microstructures of more uniform size, and Δ decreases with shear rate. Eventually, the two descriptions are interrelated but made from different points of view, since modified interparticle interactions in mixtures is accompanied by changes in the flocculation characteristics of the particles in connection with the degree of polydispersity.

4. Conclusions

The shear rate dependence on viscosity of magnetic particle suspensions is well described by the Casson equation. For different types of particles, the magnitude of yield stress is: $CrO_2 \sim \gamma$-$Fe_2O_3 > \alpha$-$Fe_2O_3 >$ Ba-ferrite. The observation of the consistent trend between the intrinsic viscosity obtained by Mooney's equation and yield stress by the Casson equation is natural, since the former incorporates changes in measured viscosity into the intrinsic viscosity, whereas the latter incorporates changes into the yield stress. The highest yield stress for Ba-ferrite among the four types of particles represents the sensitive flocculation characteristics of Ba-ferrite with concentration very well. Intrinsic viscosity obtained by fitting to Mooney's equation was used to obtain the $[\eta]_\infty$ values: $\sim$26(CrO_2, γ-Fe_2O_3) > 22(α-Fe_2O_3) > 12(Ba-ferrite). The trend of $[\eta]_\infty$ value is in accord with the primary particle characteristics: the largest value for both CrO_2 and γ-Fe_2O_3 accounts for the rod-like magnetic particle nature, the slightly lower value of α-Fe_2O_3 for rod-like but non-magnetic characteristics, and the smallest value of Ba-ferrite for its plate-like shape. In addition, mixtures of γ-Fe_2O_3 and α-Fe_2O_3 particle suspensions led to a negative deviation from the tie line of the viscosities of individual particle suspensions. As indicated in the discussion, numerous factors need to be improved in the rheological characterization of particle suspensions. Ultimately, more refined theoretical developments for suspensions subject to flocculation are necessary.

Acknowledgement

This work was partially supported by the Korea Science and Engineering Foundation (GRANT No. 981-1109-049-2).

References

1. M. P. SHARROCK, *IEEE Trans. Magn*. **Mag-25** (1989) 4374.
2. T. E. KARIS and M. S. JHON (Eds.), *Colloids and Surfaces A: Physicochem. Eng. Aspects* **80**(1) (1993).
3. T. L. SMITH and C. A. BRUCE, *J. Colloid Interface Sci*. **72** (1979) 13.
4. I. M. KRIEGER, *Adv. Colloid Interface Sci*. **3** (1972) 111.
5. V. V. JINESCU, *Intern. Chem. Eng*. **14** (1974) 397.
6. G. B. JEFFERY and A. ACRIVOS, *AIChE J*. **22** (1976) 417.
7. A. MEWIS and J. B. SPAULL, *Adv. Colloid Interface Sci*. **6** (1976) 173.
8. R. V. MEHTA, P. PRABHAKARAN and H. I. PATEL, *J. Magn. Magn. Mater*. **39** (1983) 35.
9. M. C. YANG, L. E. SCRIVEN and C. W. MACOSKO, *J. Rheol*. **30** (1986) 1015.
10. P. N. KUIN, *IEEE Trans. Magn*. **Mag-23** (1987) 97.
11. S. DASGUPTA, *J. Colloid Interface Sci*. **121** (1988) 208.
12. *Idem*., *ibid*. **124** (1988) 22.
13. M. S. JHON, T. M. KWON, H. J. CHOI and T. E. KARIS, *Ind. Eng. Chem. Res*. **35** (1996) 3027.
14. T. E. KARIS and M. S. JHON, *Proc. Natl. Acad. Sci*. (USA) **83** (1986) 4973.
15. T. M. KWON, M. S. JHON and T. E. KARIS, *IEEE Trans. Instrum. Meas*. **41** (1992) 10.
16. T. M. KWON, M. S. JHON, H. J. CHOI and T. E. KARIS, *Colloids and Surfaces* **80** (1993) 39.
17. T. M. KWON, P. L. FRATTINI, L. N. SADANI and M. S. JHON, *ibid*. **80** (1993) 47.
18. H. J. CHOI, Y. D. PARK, P. L. FRATTINI and M. S. JHON, *J. Appl. Phys*. **75** (1994) 5579.
19. T. M. KWON, M. S. JHON and H. J. CHOI, *J. Molecular Liq*. **75** (1998) 115.
20. *Idem*., *Mater. Chem. Phys*. **49** (1997) 225.
21. N. CASSON, in "Rheology of Disperse Systems," edited by C. C. Mill (Pergamon Press, N. Y., 1959).
22. G. BOTTONI, D. CANDOLFO, A. CERCHETTI and F. MASOLI, *IEEE Trans. Magn*. **Mag-8** (1972) 770.
23. A. A. POTANIN and N. B. UR'EV, *Colloid J. of USSR* **53** (1991) 42.
24. J. S. CHONG, E. B. CHRISTIANSEN and A. D. BAER, *J. Appl. Ploym. Sci*. **15** (1971) 2007.
25. R. J. FARRIS, *Trans. Soc. Rheol*. **12** (1968) 281.

Received 2 February
and accepted 11 August 1999